SCIENCE CHINA
Chemistry

•MINI REVIEWS•
SPECIAL TOPIC: Aggregation-induced Emission

August 2018 Vol.61 No.8: 882–891
https://doi.org/10.1007/s11426-018-9300-5

Biothiol-specific fluorescent probes with aggregation-induced emission characteristics

Siyang Ding, Mengjie Liu & Yuning Hong*

Department of Chemistry and Physics, La Trobe Institute for Molecular Science, La Trobe University, Melbourne, Victoria 3086, Australia

Received April 3, 2018; accepted June 5, 2018; published online July 18, 2018

Biothiols are important species in physiological processes such as regulating protein structures, redox homeostasis and cell signalling. Alternation in the biothiol levels is associated with various pathological processes, therefore non-invasive fluorescent probes with high specificity to biothiols are highly desirable research utilities. Meanwhile, fluorescent probes with aggregation-induced emission properties (AIEgens) possess unique photophysical properties that allow modulation of the sensing process through controlling the aggregation-disaggregation or the intramolecular rotational motions of the fluorophores. Herein we review the recent progress in the development of biothiol-specific AIEgens. In particular, the molecular design principles to target different types of biothiols and the corresponding sensing mechanisms are discussed, along with the potential of the future design and development of multi-functional bioprobes.

biothiols detection, aggregation-induced emission, fluorescent probes, bioimaging, biosensing

Citation: Ding S, Liu M, Hong Y. Biothiol-specific fluorescent probes with aggregation-induced emission characteristics. *Sci China Chem*, 2018, 61: 882–891, https://doi.org/10.1007/s11426-018-9300-5

1 Introduction

Biological thiol-containing molecules (biothiols), including cysteine (Cys), homocysteine (Hcy), glutathione (GSH), and hydrogen sulfide (H_2S), are essential biomolecules that play a critical role in numerous physiological processes, such as redox homeostasis, cell signalling and detoxification [1–3]. Abnormal concentrations of biothiols have been reported to associate with many medical conditions. For example, elevated levels of labile Cys may be involved in neurodegeneration whereas low Cys levels may lead to growth retardation, hair depigmentation, liver damage, skin lesions and weakness [4–9]. Hcy, the homologue of Cys with one more methylene group, is implicated in vascular and renal diseases [9]. High concentration of Hcy in blood may be a risk factor for cardiovascular and Alzheimer's disease, neural tube defects, complications during pregnancy, inflammatory bowel disease and osteoporosis [10,11]. GSH, the most abundant thiolated tripeptide, is an important antioxidant that regulates the intracellular buffering system. By scavenging the reactive oxygen species (ROS) and free radicals, GSH prevents cells from damage caused by oxidative stress and toxins. GSH also participates in affecting the effectiveness of chemotherapy [12–14]. H_2S, a well-known poisonous and flammable gas, has critical biological functions. It is an important endogenous gaso-transmitter with relatively high concentration in the brain. It is involved in learning and memory, regulation of blood pressure, inflammation as well as metabolism [15]. Abnormal concentration of H_2S has been found in conditions such as Alzheimer's disease and diabetes [16]. It can also bind to iron in the mitochondrial cytochrome enzymes and lead to apnea asphyxiate.

To date, there have been many analytical methods developed for biothiol detection, such as high-performance liquid chromatography (HPLC) [17–19], mass spectrometry (MS)

*Corresponding author (email: Y.Hong@latrobe.edu.au)

and capillary electrophoresis [20]. These methods, however, suffer from disadvantages such as invasive, complicated and expensive instruments, and laborious sample separation/purification. In recent years, fluorescence-based analytical technologies have attracted substantial interest as they are non-invasive and capable of real-time monitoring of biological events both *in vitro* and *in vivo*. To employ such techniques for biothiol detection, the availability of fluorescent probes with high specificity and sensitivity is the prerequisite.

To target biothiols, the most straightforward way is to make use of the strong nucleophilic property of the thiol group. A number of thiol-based reactions that readily occur in mild conditions can be applied in the design strategies (Figure 1). Examples include cyclisation with aldehydes [21], Michael addition at α,β-unsaturated carbonyl moieties [22,23], cleavage of sulfonamide and sulfonate esters [24,25], conjugate addition cyclisation with acrylates [26,27], aromatic substitution rearrangement [28] and native chemical ligation [29].

A major shortcoming associated with the earlier generation of biothiol-specific probes is that they are generally derived from those conventional fluorescent dyes, which are strongly emissive when solubilised in organic solvents but quenched in biological aqueous environment where they aggregate due to poor solubility. This phenomenon is known as aggregation-caused quenching (ACQ). In biological settings, this undesirable effect can be especially problematic when high probe concentration is required, or multiple reactive sites are present in a single biomolecule of interest. In 2001, Tang *et al.* [30] found an opposite luminescence phenomenon to the ACQ effect. Such molecules exhibit no or only weak emission in the solubilised state, but become progressively emissive upon forming aggregates. This distinctive phenomenon was denominated "aggregation-induced emission (AIE)", which has been attracting increasing attention since it provides a powerful and versatile strategy for designing new generation probes that eliminate the aforementioned problems. By harnessing the unique AIE feature, a wide range of bioprobes have been developed, for example, for following protein aggregation in neurodegenerative disease models [31], for detecting apoptosis in cells [32], for monitoring telomerase activity in cancer diagnosis [33], and for following ROS in inflammatory and normal cells [34]. Mechanistic studies have attributed the AIE phenomenon to the restricted intramolecular rotation (RIR) of the aromatic moieties [35]. When the AIE-active molecules (AIEgens) form aggregates, the intramolecular rotation is suppressed and the π-π interaction inhibits the excitonic non-radiative transition, resulting in activation of strong emission. Such process can also be used to modulate the fluorescence behaviour of AIEgens. In general, interacting with analytes that induce aggregation or disaggregation of the AIEgens can lead to enhanced or weakened fluorescence respectively. In this respect, biothiol-specific probes derived from AIE-active scaffolds have the capability of visualising and quantitatively measuring biothiols with wide range of concentration, as well as proteins that contain multiple free cysteine moieties. Examples of well documented AIE-active scaffolds include the tetraphenylethene (TPE) and silole derivatives [36]. Through introduction of thiol-reactive moieties onto these scaffolds, a series of novel thiol-specific AIEgens have been developed.

In this review, by illustrating some symbolic examples, we

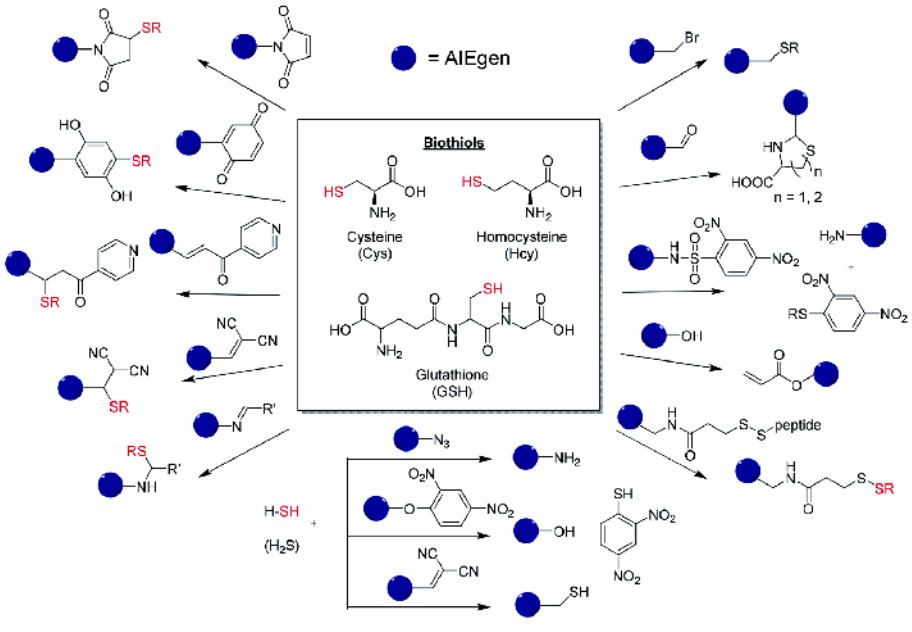

Figure 1 Chemical reactions involved in the detection mechanism of biothiol-specific fluorescent probes (color online).

aim to briefly summarise the recent progress in the development of biothiol-specific AIEgens. In particular, we highlight the principles in the molecule design strategies and their biological applications where available.

2 AIE-active Cys/Hcy/GSH probes

2.1 Thiol-reactive AIEgens based on derivatisation

The robust Michael addition reaction can readily occur under mild conditions and has been widely applied in designing thiol-specific probes for protein labelling. Several thiol-reactive groups have been engaged, among which the maleimide (MI) group is the one that has been extensively explored due to its high specificity. Tang *et al.* [37] reported the first example of thiol-specific probe, TPE-MI (**1**). Introducing the MI group quenched the fluorescence of the TPE core, rendering the whole molecule non-emissive in both solution and aggregate state. This quenching effect was attributed to the exciton annihilation process associated with the n-π electronic conjugation of the carbonyl (C=O) and olefinic (C=C) groups. Model reactions proved that when thiol was added, a thiol-ene hydrothiolation reaction could occur rapidly at ambient condition, where the thiol group conjugated onto the C=C double bond in the MI moiety, breaking the n-π conjugation and recuperating the AIE effect. As a result, **1** was applied as a "light-up" probe for selective detection of Cys on a TLC plate. When excited at 365 nm, only the Cys spot rapidly emitted bright blue light when **1** was applied, while other amino acids remained non-emissive. This technique was proven to be sensitive to Cys from 1 to 100 ng/mL, as well as GSH. **1** Showed good cell permeability and no cytotoxicity, and this supports its potential application in mapping the level of intracellular thiols.

In aqueous media, **1** was non-emissive even when conjugated with free thiols. A probable explanation for this observation is that conjugation to small and soluble biothiols could not sufficiently constrain the intramolecular motion of the TPE core, failing to trigger its fluorescence. This unique AIE feature endows **1** with the ability to detect unfolded proteins, even in the intracellular environment where GSH is abundantly present. Cys residues are usually buried in folded proteins, but become exposed on protein surface when the proteins unfold. Based on this idea, Hong, Hatter and coworkers [38] demonstrated the use of **1** to report the change in cellular unfolded protein load. Disruption of the cellular protein homeostasis (proteostasis) can promote protein unfolding, which in turn results in accumulation of aggregated proteins (Figure 2(a)). Such process has been associated with many medical conditions, especially in neurodegenerative diseases.

1 is the first chemical probe reported for measuring unfolded proteins as a reflection of proteostasis capacity in live cells without expressing exogenous proteins. Confocal microscopy images (Figure 2(b)) showed that **1** was concentrated in the region of endoplasmic reticulum (ER), the anticipated major location of protein synthesis and folding. By applying a variety of stressors to proteome foldedness, including heat shock (Figure 2(c, d)), tunicamycin (Figure 2(e)), inhibition of hub chaperone Hsp90 with novobiocin, and hydrogen peroxide (Figure 2(f)), the fluorescence intensity was enhanced in comparison with the control cells. **1** was also applied in monitoring the collapse of proteostasis in stem cells derived from Huntington's disease patients and model cells that express mutant proteins. Furthermore, **1** was capable in detecting protein damage in malaria parasites treated with a frontline anti-malaria drug, dihydroartemisinin (DHA).

Similar to maleimide, benzoquinone (BQ) can also react with thiols via Michael addition reaction. Chi *et al.* [39] reported a TPE-based probe that incorporates a BQ moiety. TPE-BQ (**2**, Figure 3) exhibited fluorescence turn-on upon reacting with thiols. Density functional theory calculations illustrated the complete separation of the electron delocalisation of highest occupied molecular orbital (HOMO) and lowest unoccupied molecular orbital (LUMO). This suggested that the fluorescence quenching was originated from a photo-induced intramolecular charge transfer (PICT) process. When the BQ unit reacted with thiols, it became a hydroquinone and the PICT process was interrupted, leading to fluorescence enhancement. Meanwhile, the change in conjugation also caused alternation in the UV-Vis spectra, which enabled "naked eye" Cys detection. **2** could react with Cys rapidly, thus enabled real-time Cys tracking in 30 s with a detection limit of 0.88 μM.

Michael addition can also occur between a thiol and an α,β-unsaturated carbonyl/ketone moiety. Tang *et al.* [40] reported a TPE-based probe linked to a pyridine ring (TPE-Py, **3**, Figure 3) via an α,β-unsaturated ketone. Upon adding biothiols, the unsaturated ketone is undermined, resulting in the disruption of molecular backbone conjugation and subsequent change in emission. In the detection medium comprised of acetonitrile/phosphate buffer (20:80 *v*/*v*, 20 mM, pH 8), **3** displayed a strong yellow emission at 550 nm. Interestingly, addition of Hcy induced an obvious blue-shift to 455 nm, whereas Cys and GSH only caused a drastic decrease in emission intensity. This suggested that **3** can be used as a selective probe for Hcy detection, where the detection limit was found to be 0.346 μM, well covering the physiological level of plasma Hcy.

The aforementioned thiol-ene click reaction can also occur at an unsaturated double bond conjugated to other electron-withdrawing moieties. For example, Tang *et al.* [41] reported the probe TPE-Cy (**4**) comprised of a TPE scaffold and an electron-withdrawing hemicyanine unit. This probe has been found capable of differentiating Hcy over Cys, GSH and

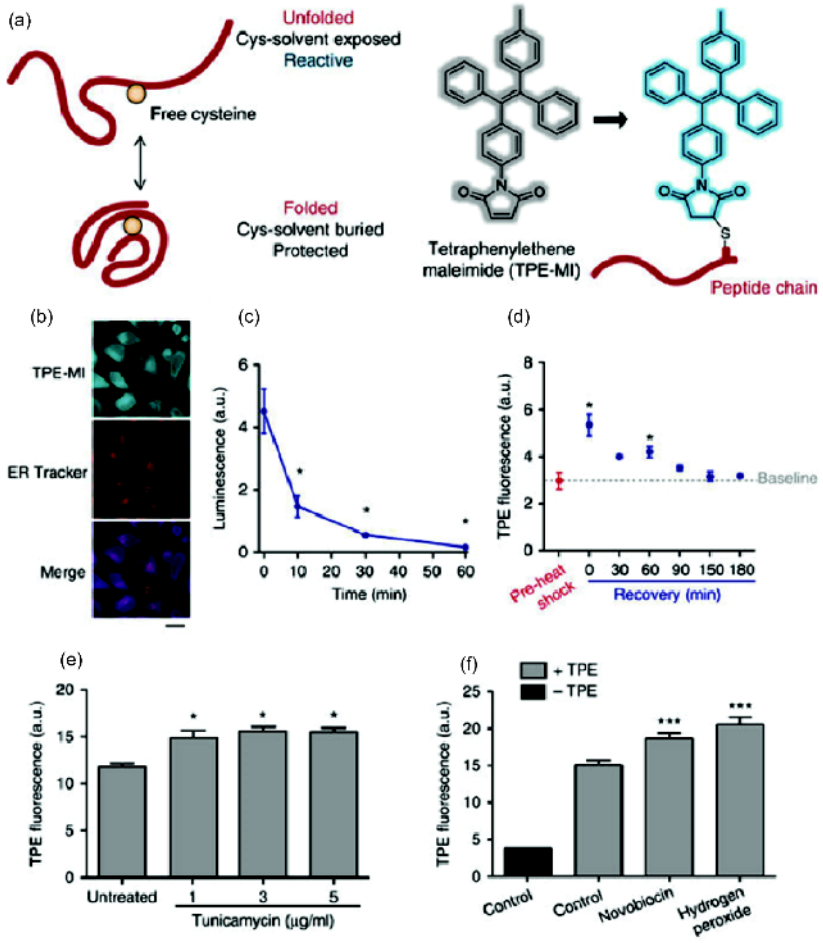

Figure 2 (a) Strategy for assaying protein foldedness via access to buried Cys thiols utilising TPE-MI; (b) confocal microscopy images for TPE-MI staining of HeLa cells with ER Tracker counterstain; (c) unfolding of the proteome by heat shock as assessed by denaturation of Renilla luciferase and luciferase activity; (d) heat shock treatment of HeLa cells at 42 °C for 45 min and subsequent time course of recovery at 37 °C; (e) effect of overnight tunicamycin treatment on HeLa cells; (f) effects of hsp90 inhibitor novobiocin (800 μM for 6 h) and free radical generator, hydrogen peroxide (100 μM for 1 h) on HEK293 cells [38] (color online).

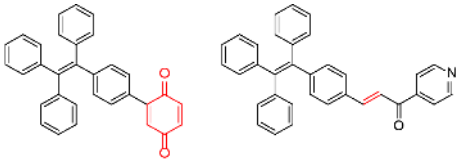

Figure 3 Molecular structures of probes **2** and **3** (color online).

other amino acids. After adding Hcy, the red emission of **4** alone in pH 8 buffer was suppressed while a strong blue emission appeared. In the case of Cys, only very weak blue emission was observed. NMR analysis demonstrated that the thiol group reacted with the double bond (highlighted in Figure 4) via a 1,4-addition, which was preferential for the less sterically hindered Hcy. On the other hand, the bulky GSH was the least reactive one thus no obvious change in emission could be observed (Figure 4).

The strong electron-withdrawing malonitrile group has been incorporated in the probe TPE-DCV (**5**, Figure 5) [42], which reacts with biothiols via the thiol-ene click reaction. **5** showed fluorescence turn-on effect selectively with GSH but not Cys, Hcy or other amino acids in the detection medium (water:ethanol=68%:32%, *v*/*v*). It was speculated that GSH, but not Cys or Hcy, could induce a significant increase in hydrophilicity, causing aggregation and emission of the **5**-GSH adduct. **5** could also be used as a label-free sensor for the activity of glutathione reductase, which cleaves GSSG to produce GSH so as to regulate the redox balance. The similar design strategy has also been applied in the malonitrile-containing silole derivative by Tang *et al.* [43]. The probe DMTPS-*p*-DCV (**6**, Figure 5) could differentiate GSH from Cys and Hcy in terms of distinct kinetic, while DMTPS-*m*-DCV (**7**, Figure 5) with the substitution on the meta-position showed high selectivity to Cys with a detection limit as low as 0.5 μM. The underlying mechanism can be attributed to their molecular structures and the solubility of the probe-thiol adducts.

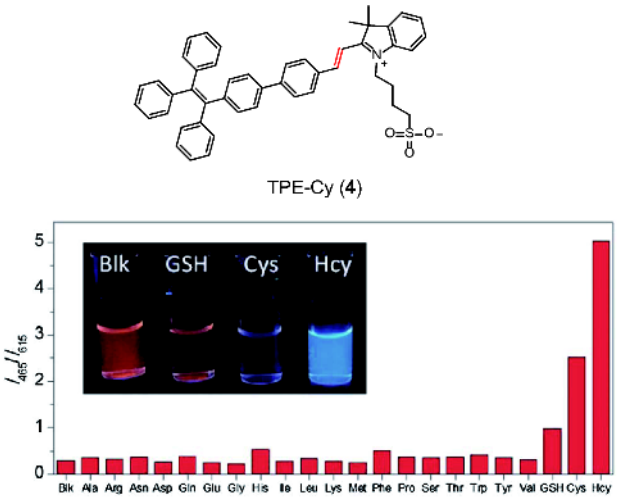

Figure 4 Emission ratio changes of probe **4** (10 μM) upon addition of 1 mM different amino acids or GSH in pH buffer. Inset: solution of 10 μM **4** in blank buffer or 100 mM GSH, Cys and Hcy (left to right) under UV lamp; molecular structure of probe **4** [41] (color online).

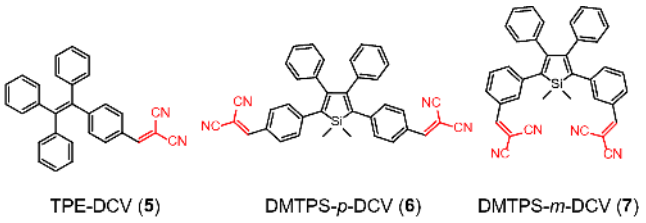

Figure 5 Molecular structures of probes **5**, **6**, and **7** (color online).

Another thiol-specific electrophilic group is the C=N double bond of the Schiff base. Xia, Tang *et al.* [44] synthesised a Schiff base-bearing TPE-coumarin hybrid (TPE-Cou, **8**, Figure 6) as a fluorescence turn-on probe. **8** exhibited weak emission at 487 nm in THF solution owing to the strong photo-induced electron transfer (PET) process of the Schiff base C=N bond, as well as the active intramolecular rotation of the TPE core. The HOMO and LUMO of **8** have been calculated to prove the above inference, suggesting that the coumarin unit and the C=N linker both play key roles in determining the photoluminescence (PL) properties. Unlike most TPE derivatives that are strongly emissive in solid state, the aggregate of **8** was only weakly fluorescent. Its crystal structure revealed that the whole molecule had a coplanar and rigid configuration. This led to the multiple π-π stacking interactions and PET process of the Schiff base, causing fluorescence quenching and red-shift in emission (590 nm). When exposed to thiols, the TPE core allowed the nanoaggregates to emit strongly at 473 nm as the PET process was blocked. The sensing mechanism was attributed to the conjugation addition involving thiol and the Schiff base unit, which breaks the C=N double bond and undermines the through-bond conjugation of the overall molecule. The

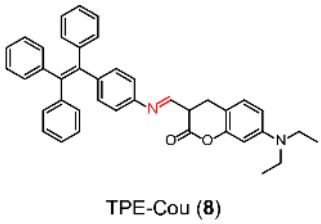

Figure 6 Molecular structure of probe **8** (color online).

sensitivity of this probe to Cys, Hcy and GSH was investigated by fluorescence titration, and an excellent linear relationship between the PL intensity ratio and Cys concentration (5−500 μM) was established. This suggested the suitability of **8** for quantitative detection of Cys. In addition, this probe was highly specific to Cys and Hcy, which produced almost 30-fold enhancement in emission. However, the relatively bulky GSH could hardly enter the inner cavities of the nanoaggregates, resulting in lower reactivity compared to Cys and Hcy.

A similar mechanism was also seen in the CPA probe (**9**, Figure 7) developed by Qi *et al.* [45]. Different from the turn-on phenomenon observed for **8**, this probe exhibited a notable blue-shift in emission (from 575 to 450 nm) when exposed to Cys (Figure 7). Evaluation of its specificity and anti-jamming capability to Cys has indicated that this probe is a promising colorimetric chemosensor. Moreover, a linear relationship between the PL intensity and Cys concentration in the range of 1–13 μM was obtained, which suggested that **9** is an excellent ratiometric Cys probe.

In addition to the aforementioned examples, alkyl halide, such as the bromomethyl moiety, is another functional group capable of covalently labelling biothiols. Tang *et al.* [46] reported their TPE derivative 1-[4-(bromomethyl)phenyl]-1,2,2-triphenylethene (**10**) and successfully applied it in specifically pre-staining Cys-bearing proteins in sodium dodecyl sulfate polyacrylamide gel electrophoresis (SDS-PAGE, Figure 8). Comparing with the commercial dye Coomassie brilliant blue (CBB) utilised in protein staining, **10** could selectively target BSA (35 Cys) and yeast enolase (1 Cys) but not horse myoglobin (0 Cys). The AIE property of **10** led to fluorescence enhancement at 480 nm in aggregated state, which showed 3-fold increase in emission after reacting with the free thiol groups. This phenomenon was attributed to the elimination of internal heavy atom effect of bromide that was substituted by thiols, which increased the signal-to-noise ratio and enabled the effective application in pre-staining SDS-PAGE gel.

Another approach to thiol detection through conjugation is the cyclisation with aldehydes. Sun, Tang *et al.* [47,48] prepared a series of aldehyde-functionalised TPE- and silole-based probes (**11**, **12** and **13**, Figure 9), and applied them in discriminating Cys and Hcy using the distinct kinetics of

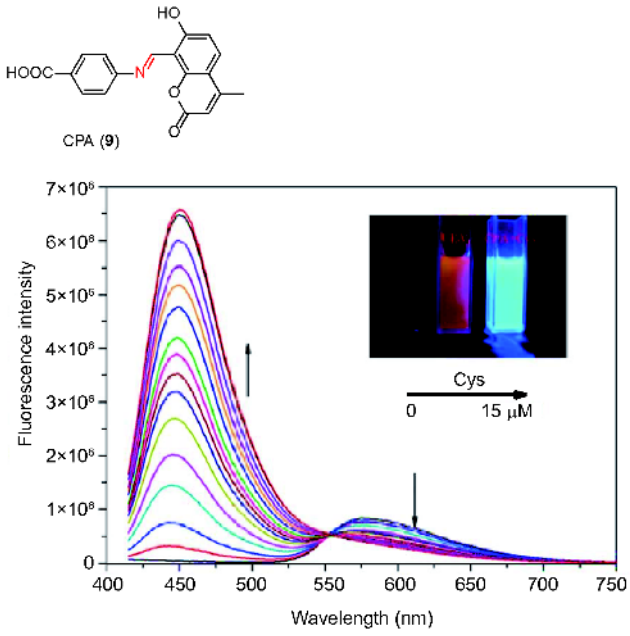

Figure 7 Fluorescence intensity changes of probe **9** (5 μM) in the presence of a gradually varied concentration of Cys (0–15 μM) in HEPES buffer. Inset: solution of **9** in blank buffer and 15 μM Cys under UV lamp; molecular structure of probe **9** [45] (color online).

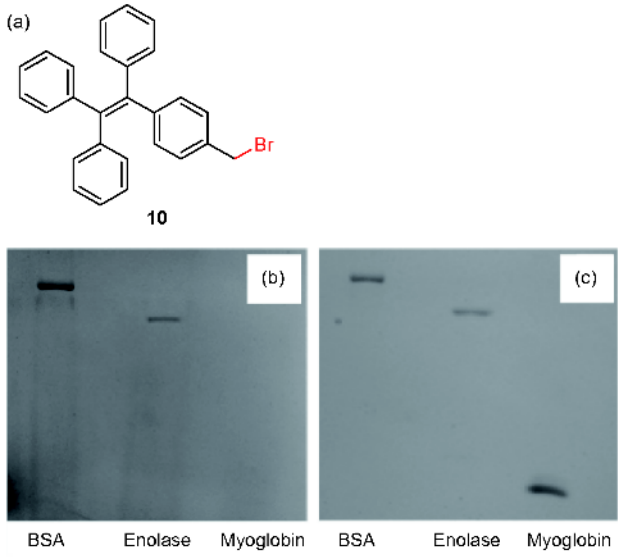

Figure 8 (a) Molecular structure of probe **10**; (b) inverted SDS-PAGE fluorescence image of **10** labeled proteins (BSA, Enolase, and Myoglobin, left to right) with various contents of Cys residue; (c) image of the same gel post-stained with Coomassie R-250 [46] (color online).

cyclisation of the thiazolidine and thiazinane rings. In this system, **11**, **12** and **13** along showed weak emission in the HEPES-DMSO mixture (*v*/*v*=50/50) owing to their moderate solubility in this medium. Upon adding Cys, the free thiol and amino groups rapidly reacted with their aldehyde moieties, turning the reaction mixture turbid due to the lowered solubility of the resulting thiazolidine derivative. The

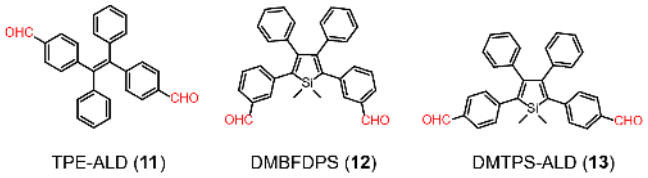

Figure 9 Molecular structures of probe **11**, **12** and **13** (color online).

fluorescence peaks of both probes exhibited marked enhancement and blue-shift. In contrast, there was little change observed when Hcy was added to the probe-containing media. Notably, probe **11** outshined the other two probes in performance in terms of faster response and greater emission enhancement, implying that it could be applied as a potential indicator for Cys deficiency. In addition, their good sensitivity, specificity and selectivity have also been demonstrated in this article.

2.2 Thiol-reactive AIEgens based on cleavage

The thiol detection mechanism of all aforementioned examples are based on derivatisation, where the biothiols are conjugated to the probes to trigger easily detectable changes in their photophysical properties. Another efficient strategy to achieve thiol detection makes use of the thiol-reactive fluorescence quenchers. For example, the widely-used 2,4-dinitrobenzenesulfonyl (DNBS) group can be conjugated to an amine-containing AIEgen to switch off its emission. The sulfamide linkage can be cleaved by the nucleophilic thiol group, and the AIEgen would become fluorescent with intensity corresponding to the concentration of the thiol(s) of interest. Based on this principle, Tong *et al.* [49] reported their salicylaldehyde azine-containing turn-on probe DNBS-CSA (**14**, Figure 10). Interestingly, the probe produced obvious response to biothiols on test papers, indicating its great potential in thiol detection on solid phase. The same design was used in TPENNO$_2$ (**15**, Figure 10) developed by Wang *et al.* [50]. Its ability in discriminatory detection of Cys over Hcy and GSH is dependent on the different reaction kinetic profiles. Another effective quencher is the acrylate group conjugated at the hydroxyl moiety, which serves as the Cys recognition site and the excited-state intramolecular proton transfer (ESIPT) blocker. This has been reflected in the design of **16**, **17**, and **18** (Figure 10) [51–53]. The acrylate group could be cleaved off by Cys in aqueous solution under mild conditions, releasing the free hydroxyl group and thus producing strong emission enhancement.

Except for modifying the core-quencher conjugation, probe-peptide conjugates have provided a novel design strategy towards turn-on probes. Liu *et al.* [54] demonstrated that conjugating the TPE core with hydrophilic peptide fragments, such as poly-aspartic acid (Asp) peptides, could

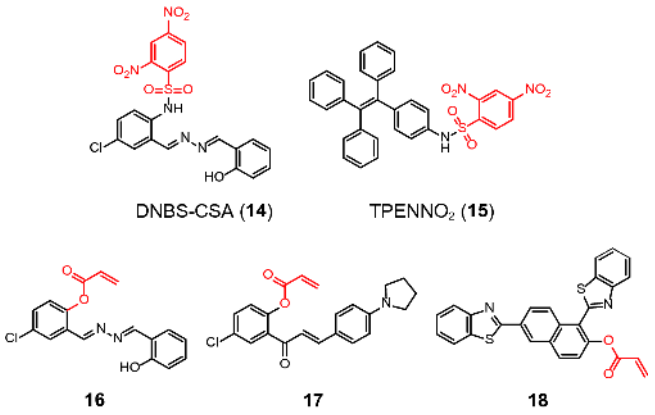

Figure 10 Molecular structures of probes **14**–**18** (color online).

fine-tune the aggregation in aqueous media and thus the AIE characteristics. They synthesised a water-soluble probe-peptide conjugate TPE-SS-D_5 (**19**, Figure 11(A)) that links a penta-Asp peptide to the TPE core via a cleavable thiol-reactive disulfide bridge. This probe was found useful in detecting GSH *in vitro*. **19** was nearly non-emissive in the DMSO/water mixture (*v*/*v*=1/199). Upon addition of GSH, the disulfide bridge was specifically cleaved, causing aggregation of the hydrophobic TPE core, which emitted at 465 nm when excited at 304 nm. A linear relationship between the PL intensity and the GSH concentration was established with a detection limit of 4.26 μM, indicating the promising application of **19** in quantificational bio-sensing. Further research introduced the cyclic RGD (cRGD) peptide as a selective targeting domain for $\alpha_v\beta_3$ integrin, a protein found in many angiogenic cancers [55]. The resulting probe TPE-SS-D5-cRGD (**20**, Figure 11(A)) exhibited strong blue emission in live cell imaging, when incubated with the human glioblastoma cell lines that over-express $\alpha_v\beta_3$ on the cell membrane. On the contrary, its precursor **19** showed nearly no response under the same condition (Figure 11(B)).

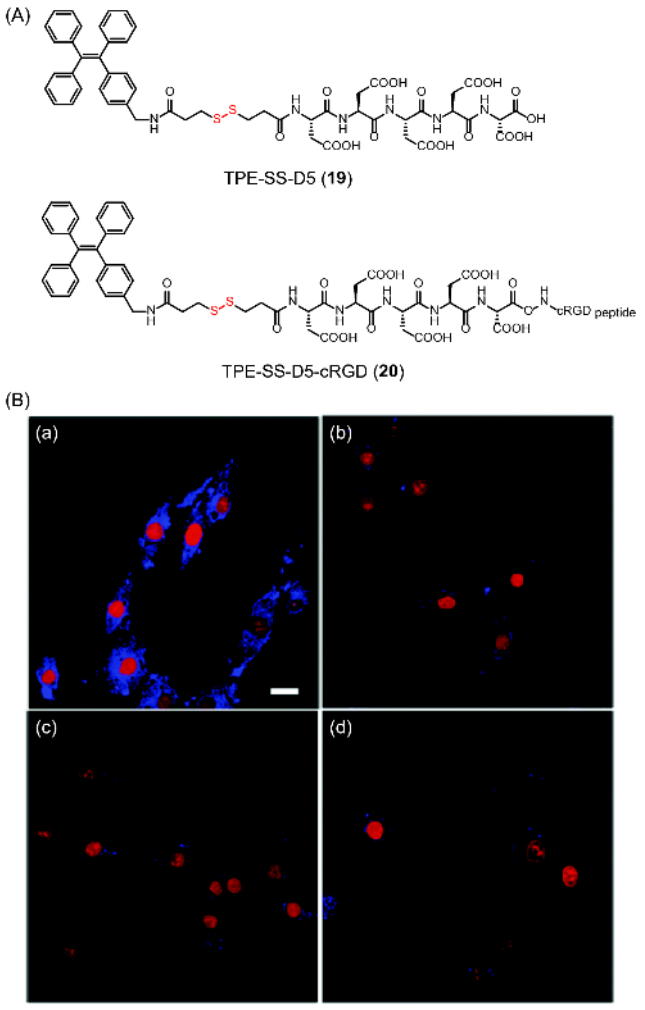

Figure 11 (A) Molecular structures of probe **19** and **20**; (B) confocal microscopy images of U87-MG (a, b) and MCF-7 (c, d) cells after incubation with **20** (a, c) and **19** (b, d). The nuclei were stained with propidium iodide [54,55] (color online).

3 AIE-active H_2S probes

Development of novel ratiometric AIEgens specific for H_2S detection has been a hot research topic, owing to the significant implications of H_2S in physiological and pathophysiological processes. A few of such probes have emerged in recent years. Notably, their detection mechanisms make use of the strong reducing power exhibited by H_2S. Tang *et al.* [56] reported a tetraphenylpyrazine (TPP)-based probe (TPP-PDCV, **21**, (Figure 12(a)) bearing an electrophilic malonitrile group as the H_2S-reactive site. **21** exhibited classical AIE characteristic in DMSO/water mixtures with various water fractions (f_w), and strong emission was observed when f_w>50%. In the medium comprised of DMSO/PBS (25 μM, *v*/*v*=9:1), **21** exhibited an orange-yellow emission peaked at 565 nm, whereas upon adding 10 eq. of NaHS (an *in situ* H_2S generator), the emission was gradually shifted to 429 nm because the donor-acceptor system was destructed. The ratio between the PL intensities at 429 and 565 nm continued increasing within 10 min, clearly revealing the detection process ((Figure 12(b)). This indicated that **21** is capable of real-time H_2S detection. A linear relationship between the PL intensity and NaHS concentration in the range 0–75 and 150–225 μM was obtained, indicating that **21** is promising for quantitative H_2S detection with a limit of 0.5 μM (Figure 12(c)). Furthermore, by analysing various anions and biothiols, **21** showed strong selectivity to H_2S compared with those previously reported non-AIE probes [57]. It was found that the probe first undergoes a nucleophilic addition with H_2S, then a possible hemolysis and hydrolysis to form the intermediate. The oxidation reaction takes place quickly between the intermediates, generating the

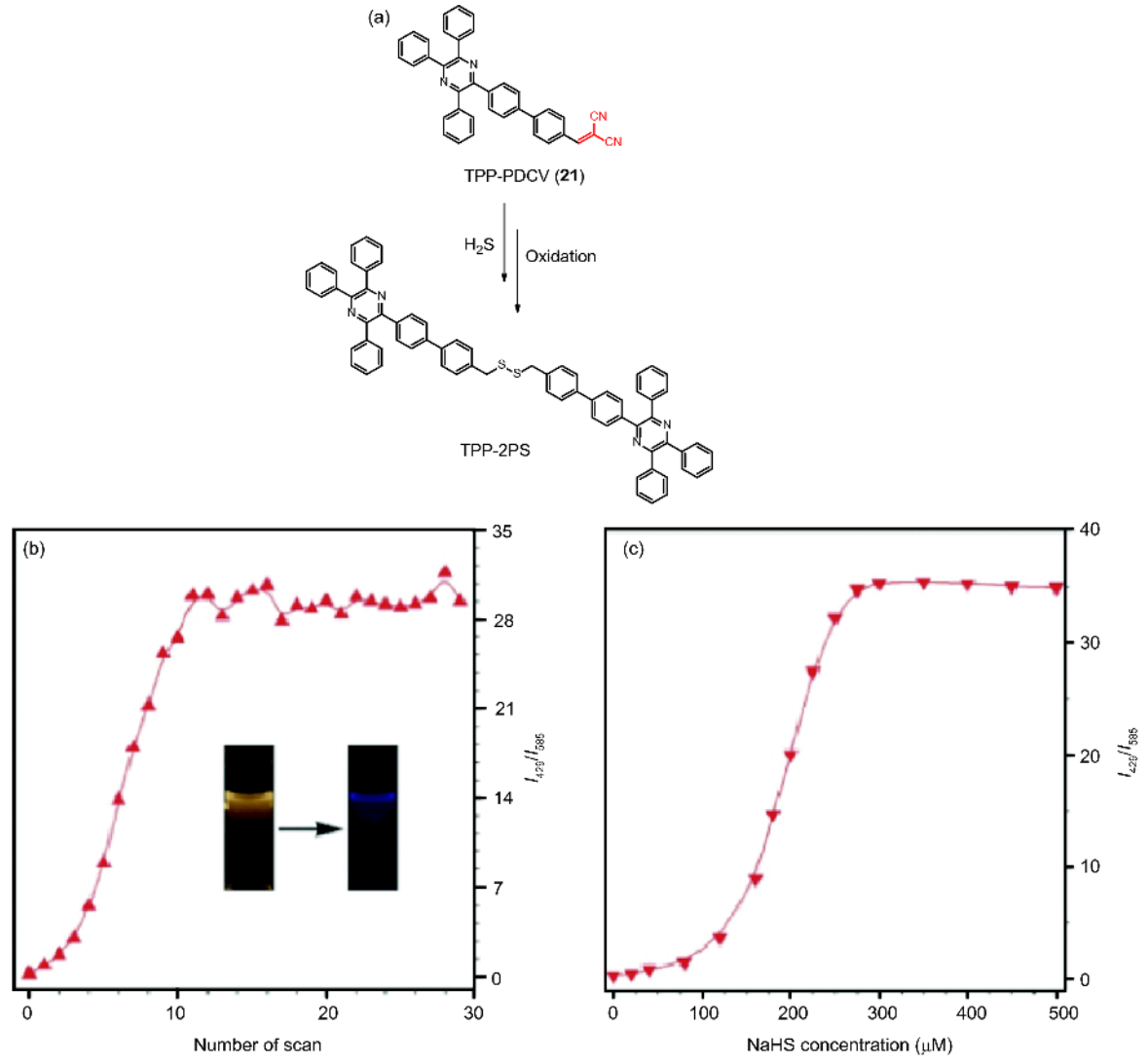

Figure 12 (a) H_2S detecting mechanism of **21**; (b) plot of PL intensity ratio versus the number of scan in a total time of 25 min. Inset: fluorescence of **21** before and after reacting with NaHS; (c) plot of PL intensity ratio versus NaHS concentration [56] (color online).

dimer as a final product (Figure 12(a)).

Measuring the cellular level of H_2S *in vivo* is another great challenge. To address this problem, Tang *et al.* [58] reported a dual signaling probe TPE-NP (**22**, Figure 13(a)) that consists of the TPE core and two dinitrophenyl ether (NP) moieties. Due to the electron transfer between the TPE and NP unit, the whole molecule showed no absorption and emission in visible region. However, when H_2S was added to the aqueous solution of **22**, both absorption (450 nm) and emission (480 nm) enhancement were observed instantly, resulting in prompt color changes of solution. Addition of various anions and sulfur-containing analytes did not lead to the above response, suggesting the excellent selectivity of **22** towards H_2S. Live cell imaging (Figure 13(b)) clearly showed that the H_2S level elevated with time under starvation, suggesting that **22** is an ideal tool to further investigate H_2S level *in vivo* under physiological conditions.

The azide group can be reduced to amine in the presence of H_2S, and this was made use of in TPE-Az (**23**) reported by Tang *et al.* [59]. This simple probe showed no emission in solution or aggregation state. However, it could be reduced by H_2S into the emissive product TPE-AM (Figure 14). **23** has also been developed into a facile tool for direct measurement of the H_2S concentration in various biological systems.

4 Conclusions and further perspectives

In this review, we have discussed a number of AIEgens specific for biothiol detection. Taking advantage of the strong nucleophilic characteristics of thiols, Michael addition across an unsaturated bond has been the most widely applied mechanism in biothiols detection. Cleavage of

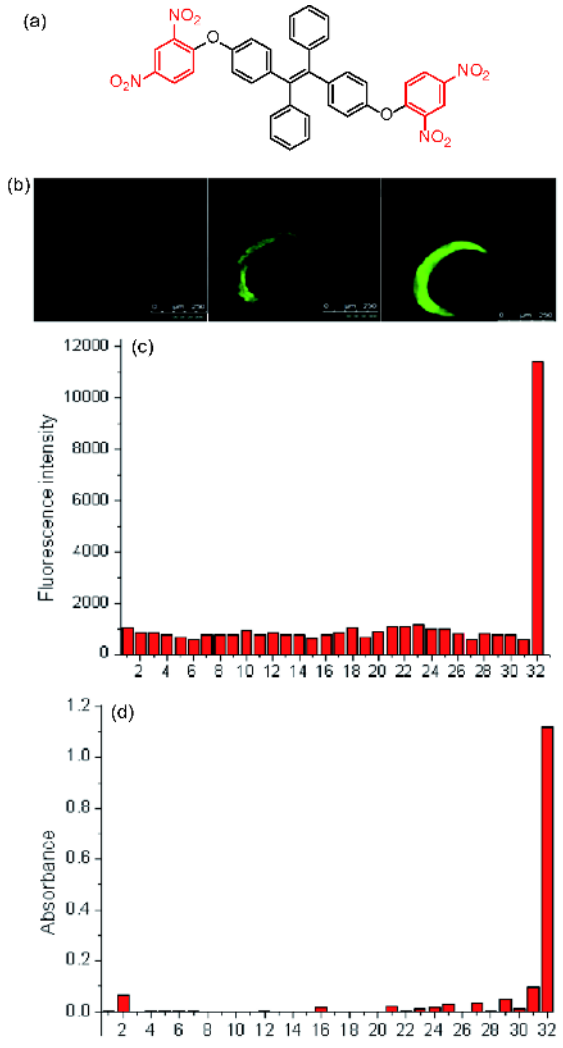

Figure 13 (a) Molecular structure of **22**; (b) fluorescence images of H_2S: **22**-loaded *C. elegans*, sensor for H_2S under stimulation with SNP, and **22**-loaded zebrafish stimulated with H_2S. (c) Fluorescence and (d) absorbance responses of 10 mM TPE-NP to various analytes in aqueous solution: (1) control, (2) I^-, (3) Br^-, (4) Cl^-, (5) CO_3^{2-}, (6) HCO_3^-, (7) $H_2PO_4^-$, (8) HPO_4^{2-}, (9) NO_3^-, (10) VC, (11) Zn^{2+}, (12) Mg^{2+}, (13) K^+, (14) Ca^{2+}, (15) Ac^-, (16) $S_2O_3^{2-}$, (17) $S_2O_4^{2-}$, (18) $S_2O_5^{2-}$, (19) SO_3^{2-}, (20) SO_4^{2-}, (21) ButOOH, (22) ClO^-, (23) H_2O_2, (24) NO, (25) O_1, (26) O_2, (27) OH^-, (28) $ONOO^-$, (29) GSH, (30) Hcy, (31) S^{2-}, (32) HS^- [58] (color online).

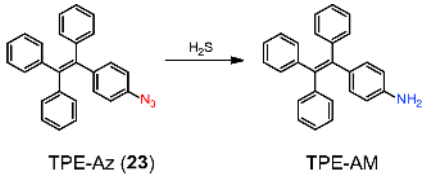

Figure 14 The reduction reaction of **23** by H_2S (color online).

fluorescence quenchers through displacement is another approach to design turn-on thiol probes. Besides, disulfide cleavage and azide reduction have also been exploited in the GSH and H_2S detection, respectively. All probes discussed here exhibit remarkable optical properties in the media upon addition of the analytes of interest, providing powerful tools for direct detection of biothiols. The experimental results indicate that the AIE cores play a vital role in determining the optical behaviour in the sensing process. It is notable that most of the discussed probes can be used for rational detection and the detection limits are in the range of physiological concentration of their intended target(s). Considering the critical roles of these biothiols in both physiological and pathophysiological processes, the AIEgen strategy can be generalised to perform various tasks in biological application.

However, the study on this topic still requires a much-needed boost. For example, to realise the long-term tracking of biothiols *in vivo*, AIEgens with longer excitation and emission wavelengths are in great demand in the future development. Reversible reaction-based probes will be another important area to exploit for real-time monitoring of the dynamic changes in biothiol levels, which will be undoubtedly most useful in the study of oxidative stress and related diseases.

In summary, some excellent thiol-specific AIEgens have emerged in recent years, which have demonstrated the potential as powerful tools for bio-sensing and imaging, site-specific protein labelling, as well as quantification of unfolded cellular proteins. Nevertheless, remarkable opportunities remain on the combination of rational structural design of probes and utilisation of them for visualising important biological related processes involving biothiols *ex vivo* and *in vivo*. Assays based on the AIE thiol probes are to be developed for clinical use, such as early diseases diagnosis, real-time tracking of disease progression at the molecular level, as well as pertinent drug discovery.

Acknowledgements This work was supported by Australian Research Council (DE170100058) and Rebecca L. Cooper Medical Research Foundation.

Conflict of interest The authors declare that they have no conflict of interest.

1 Hwang C, Sinskey AJ, Lodish HF. *Science*, 1992, 257: 1496–1502
2 Schulz JB, Lindenau J, Seyfried J, Dichgans J. *Eur J Biochem*, 2000, 267: 4904–4911
3 Wood ZA, Schröder E, Robin Harris J, Poole LB. *Trends Biochem Sci*, 2003, 28: 32–40
4 Mohamed MM, Sloane BF. *Nat Rev Cancer*, 2006, 6: 764–775
5 Weerapana E, Wang C, Simon GM, Richter F, Khare S, Dillon MBD, Bachovchin DA, Mowen K, Baker D, Cravatt BF. *Nature*, 2010, 468: 790–795
6 Lipton SA, Choi YB, Takahashi H, Zhang D, Li W, Godzik A, Bankston LA. *Trends Neurosci*, 2002, 25: 474–480
7 Chu PY, Liu MY. *J Funct Foods*, 2015, 18: 455–462
8 Marino SM, Gladyshev VN. *J Mol Biol*, 2010, 404: 902–916
9 Lin J, Lee IM, Song Y, Cook NR, Selhub J, Manson JAE, Buring JE, Zhang SM. *Cancer Res*, 2010, 70: 2397–2405
10 Finkelstein JD, Martin JJ. *Int J Biochem Cell Biol*, 2000, 32: 385–389
11 Nekrassova O. *Talanta*, 2003, 60: 1085–1095

12 Wu G, Fang YZ, Yang S, Lupton JR, Turner ND. *J Nutrit*, 2004, 134: 489–492
13 Townsend DM, Tew KD, Tapiero H. *Biomed Pharmacother*, 2003, 57: 145–155
14 Akerboom TP, Bilzer M, and Sies H. *J Biol Chem*, 1982, 257: 4248–4252
15 Whiteman M, Le Trionnaire S, Chopra M, Fox B, Whatmore J. *Clin Sci*, 2011, 121: 459–488
16 Papapetropoulos A, Pyriochou A, Altaany Z, Yang G, Marazioti A, Zhou Z, Jeschke MG, Branski LK, Herndon DN, Wang R, Szabó C. *Proc Natl Acad Sci USA*, 2009, 106: 21972–21977
17 Amarnath K. *Talanta*, 2003, 60: 1229–1238
18 Chen W, Zhao Y, Seefeldt T, Guan X. *J Pharmaceut Biomed Anal*, 2008, 48: 1375–1380
19 Guo XF, Wang H, Guo YH, Zhang ZX, Zhang HS. *J Chromatogr A*, 2009, 1216: 3874–3880
20 Zinellu A, Sotgia S, Scanu B, Usai MF, Fois AG, Spada V, Deledda A, Deiana L, Pirina P, Carru C. *Amino Acids*, 2009, 37: 395–400
21 Zhang X, Ren X, Xu QH, Loh KP, Chen ZK. *Org Lett*, 2009, 11: 1257–1260
22 McMahon BK, Gunnlaugsson T. *J Am Chem Soc*, 2012, 134: 10725–10728
23 Yi L, Li H, Sun L, Liu L, Zhang C, Xi Z. *Angew Chem Int Ed*, 2009, 48: 4034–4037
24 Lim CS, Masanta G, Kim HJ, Han JH, Kim HM, Cho BR. *J Am Chem Soc*, 2011, 133: 11132–11135
25 Lee MH, Han JH, Kwon PS, Bhuniya S, Kim JY, Sessler JL, Kang C, Kim JS. *J Am Chem Soc*, 2012, 134: 1316–1322
26 Wang H, Zhou G, Gai H, Chen X. *Chem Commun*, 2012, 48: 8341–8343
27 Xiong X, Song F, Chen G, Sun W, Wang J, Gao P, Zhang Y, Qiao B, Li W, Sun S, Fan J, Peng X. *Chem Eur J*, 2013, 19: 6538–6545
28 Niu LY, Guan YS, Chen YZ, Wu LZ, Tung CH, Yang QZ. *J Am Chem Soc*, 2012, 134: 18928–18931
29 Long L, Lin W, Chen B, Gao W, Yuan L. *Chem Commun*, 2011, 47: 893–895
30 Luo J, Xie Z, Lam JWY, Cheng L, Tang BZ, Chen H, Qiu C, Kwok HS, Zhan X, Liu Y, Zhu D. *Chem Commun*, 2001, 1740–1741
31 Kumar M, Hong Y, Thorn DC, Ecroyd H, Carver JA. *Anal Chem*, 2017, 89: 9322–9329
32 Shi H, Kwok RTK, Liu J, Xing B, Tang BZ, Liu B. *J Am Chem Soc*, 2012, 134: 17972–17981
33 Lou X, Zhuang Y, Zuo X, Jia Y, Hong Y, Min X, Zhang Z, Xu X, Liu N, Xia F, Tang BZ. *Anal Chem*, 2015, 87: 6822–6827
34 Cheng Y, Dai J, Sun C, Liu R, Zhai T, Lou X, Xia F. *Angew Chem Int Ed*, 2018, 57: 3123–3127
35 Parrott EPJ, Tan NY, Hu R, Zeitler JA, Tang BZ, Pickwell-Mac-Pherson E. *Mater Horiz*, 2014, 1: 251–258
36 Hong Y, Lam JWY, Tang BZ. *Chem Commun*, 2009, 1: 4332
37 Liu Y, Yu Y, Lam JWY, Hong Y, Faisal M, Yuan WZ, Tang BZ. *Chem Eur J*, 2010, 16: 8433–8438
38 Chen MZ, Moily NS, Bridgford JL, Wood RJ, Radwan M, Smith TA, Song Z, Tang BZ, Tilley L, Xu X, Reid GE, Pouladi MA, Hong Y, Hatters DM. *Nat Commun*, 2017, 8: 474
39 Li X, Zhang X, Chi Z, Chao X, Zhou X, Zhang Y, Liu S, Xu J. *Anal Methods*, 2012, 4: 3338–3343
40 Zhao N, Gong Q, Zhang RX, Yang J, Huang ZY, Li N, Tang BZ. *J Mater Chem C*, 2015, 3: 8397–8402
41 Chen S, Hong Y, Liu J, Tseng NW, Liu Y, Zhao E, Yip Lam JW, Tang BZ. *J Mater Chem B*, 2014, 2: 3919–3923
42 Lou X, Hong Y, Chen S, Leung CWT, Zhao N, Situ B, Lam JWY, Tang BZ. *Sci Rep*, 2014, 4: 4272
43 Mei J, Sun JZ, Qin A, Tang BZ. *Dyes Pigments*, 2017, 141: 366–378
44 Lou X, Zhao Z, Hong Y, Dong C, Min X, Zhuang Y, Xu X, Jia Y, Xia F, Tang BZ. *Nanoscale*, 2014, 6: 14691–14696
45 Yan L, Kong Z, Shen W, Du W, Zhou Y, Qi Z. *RSC Adv*, 2016, 6: 5636–5640
46 Yu Y, Li J, Chen S, Hong Y, Ng KM, Luo KQ, Tang BZ. *ACS Appl Mater Interfaces*, 2013, 5: 4613–4616
47 Mei J, Tong J, Wang J, Qin A, Sun JZ, Tang BZ. *J Mater Chem*, 2012, 22: 17063–17070
48 Mei J, Wang Y, Tong J, Wang J, Qin A, Sun JZ, Tang BZ. *Chem Eur J*, 2013, 19: 613–620
49 Peng L, Zhou Z, Wei R, Li K, Song P, Tong A. *Dyes Pigments*, 2014, 108: 24–31
50 Jiang G, Liu X, Chen Q, Zeng G, Wu Y, Dong X, Zhang G, Li Y, Fan X, Wang J. *Sens Actuat B-Chem*, 2017, 252: 712–716
51 Liu H, Wang X, Xiang Y, Tong A. *Anal Methods*, 2015, 7: 5028–5033
52 Li R, Yan L, Wang Z, Qi Z. *J Mol Struct*, 2017, 1136: 1–6
53 Zhou X, Guo D, Jiang Y, Gong D, Zhao X, Zhou L. *Tetrahedron Lett*, 2017, 58: 3214–3218
54 Zhang R, Yuan Y, Liang J, Kwok RTK, Zhu Q, Feng G, Geng J, Tang BZ, Liu B. *ACS Appl Mater Interfaces*, 2014, 6: 14302–14310
55 Yuan Y, Kwok RTK, Feng G, Liang J, Geng J, Tang BZ, Liu B. *Chem Commun*, 2014, 50: 295–297
56 Chen M, Chen R, Shi Y, Wang J, Cheng Y, Li Y, Gao X, Yan Y, Sun JZ, Qin A, Kwok RTK, Lam JWY, Tang BZ. *Adv Funct Mater*, 2018, 28: 1704689
57 Li H, Feng X, Guo Y, Chen D, Li R, Ren X, Jiang X, Dong Y, Wang B. *Sci Rep*, 2014, 4: 4366
58 Zhang W, Kang J, Li P, Wang H, Tang B. *Anal Chem*, 2015, 87: 8964–8969
59 Cai Y, Li L, Wang Z, Sun JZ, Qin A, Tang BZ. *Chem Commun*, 2014, 50: 8892–8895